Scientia Iranica B (2021) 28(1), 326–342

SCIENTIA IRANICA

Sharif University of Technology
Scientia Iranica
Transactions B: Mechanical Engineering
http://scientiairanica.sharif.edu

Research Note

Thermodynamic analysis of a novel solar trigeneration system

V. Beygzadeh[a,*], Sh. Khalilarya[a], I. Mirzaee[a], Gh. Miri[b], and V. Zare[a]

a. *Department of Mechanical Engineering, Faculty of Engineering, Urmia University of Technology, Urmia, P.O. Box 57155-419, Iran.*
b. *Department of Business Management, National Iranian Oil Refining & Distribution Company, Tehran, Iran.*

Received 4 February 2019; received in revised form 11 July 2019; accepted 22 October 2019

KEYWORDS
Energy efficiency;
Exergy efficiency;
Solar loop heat pipe system;
Regenerative organic Rankine cycle;
Combined cooling;
Heating and power;
Solar energy.

Abstract. Loop Heat Pipes (LHPs) are devices with high efficiency which can be used in solar systems. The main objectives of this research are to propose a novel Solar Combined Cooling, Heating, and Power (SCCHP) system based on LHP evaporator and present a thermodynamic analysis to improve the utilization of LHP in solar systems. Moreover, a parametric analysis was carried out to investigate the effect of key variable parameters on the system performance for three operation modes namely solar mode, solar and storage mode, and storage mode. The results showed that the main source of exergy destruction for both solar mode and the solar and storage mode was the solar LHP evaporator and for the storage mode, was the hot storage tank. The energy efficiency of the proposed system for the solar mode, solar and storage mode, and storage mode was 70.52%, 72.09%, and 64.77%. Furthermore, the exergy efficiency of the proposed system for the solar mode, solar and storage mode, and storage mode was 12.36%, 14.78%, and 47.45%, respectively.

1. Introduction

The use of locally available renewable resources all over the world is gaining significance and it ensures sustainable development and security of the energy supply [1]. Among renewable energy resources, solar energy has drawn considerable attention due to its nonpolluting character and inexhaustible supply [2]. It can be exploited by either thermal collectors or photovoltaic (PV) panels for heat or electricity production [3]. Solar energy is a plentiful and easy-to-use energy source that can be transformed either to electricity or useful heat [4]. Combined Cooling, Heating, and Power (CCHP) and Combined Heating and Power (CHP) systems are generally used as energy-saving methods for both fossil and renewable energies [5]. To decrease fossil fuel utilization, solar-based systems should be designed for CCHP systems [6]. In recent years, unlike conventional energy sources, these systems have attracted many more customers and emerged as a more sustainable energy solution [7]. The main disadvantages of PV solar systems are their limited availability on the market, high initial cost, occupation of a relatively large area for installation, and high dependence on technology development [8]. Table 1 presents an overview and a comparison of Concentrated Solar Power (CSP) technologies [7].

While conventional PV and solar thermal systems

*. *Corresponding author.*
E-mail addresses: *v_beygzadeh89@ms.tabrizu.ac.ir (V. Beygzadeh); sh.khalilarya@urmia.ac.ir (Sh. Khalilarya); i.mirzaee@urmia.ac.ir (I. Mirzaee); gholamreza.miri@gmail.com (Gh. Miri); v.zare@uut.ac.ir (V. Zare)*

doi: 10.24200/sci.2019.52866.2922

Table 1. Overview and comparison of Concentrated Solar Power (CSP) technologies.

CSP type	Parabolic troughs	Linear fresnel reflectors	Solar towers	Solar towers parabolic dish
Annual solar to electricity efficiency (%)	11–16	13	7–20	12–25
Temperatures (°C)	350–550	390	250–565	550–750
Advantages	1- The most mature CSP technology 2- Heat production at higher temperatures	1- More concentration of sunlight 2- Cheaper than the parabolic through collectors	1- Enhanced efficiency 2- Electricity generation in the absence of the sun	1- Higher efficiency 2- The most efficient systems
Disadvantages	Restriction of the output to moderate steam as a result of using oil-based heat transfer media	1- Less efficient 2- Difficult to integrate storage capacity into their design	1- Economically justified 2- Need for a large area of land 3- Daily maintenance	1- High cost 2- Lack of flexibility 3- Need for a large number of equipments for heat transfer

have their advantages and disadvantages, the Loop Heat Pipes (LHPs) enjoy several advantages, as listed in the following:

- They do not contain any mechanically movable parts and do not consume any additional energy [9];
- Their capacity may reach thousands in watts [9];
- Application of LHPs in energy-efficient systems to the recovery of low potential heat is highly probable [9];
- They are simple devices with no moving parts and can transfer large quantities of heat over long distances [10];
- They increase the life expectancy of the solar system because they can eliminate the freezing and corrosion phenomena occurring in the Solar Loop Heat Pipe Systems (SLHPS).

Shafieian et al. [11] reviewed several strategies to improve the thermal performance of heat pipe solar collectors in solar systems. They also evaluated the performance of a heat pipe solar water heating system [12]. Allouhi et al. [13] studied the forced circulation solar water heating system using heat pipe flat plate collectors. Li and Sun [14] carried out performance optimization and benefit analysis of a PV loop heat pipe/solar-assisted heat pump water heating system. Diallo et al. [15] carried out an energy performance analysis of a novel solar Photovoltaic Thermal (PVT) LHP by employing a micro channel heat pipe evaporator and a Phase Change Material (PCM) triple heat exchanger. Lu and Wang [16] carried out a thermodynamic performance analysis of Solar Combined Cooling, Heating, and Power (SCCHP) systems. Hands et al. [17] conducted a performance analysis of an SCCHP system in a building. They showed that the heat obtained from solar energy contributed consistently to reducing gas usage. Wang et al. [18] performed a thermodynamic performance analysis and optimization of an SCCHP system. They indicated that the integration of solar PV into the CCHP system would considerably improve the exergy efficiency. Yuksel et al. [19] performed a thermodynamic analysis of a novel solar system and showed that an increase in the Solar Radiation Intensity (SRI), temperature of the inner surface of absorber pipes, and concentration of ammonia in working fluid mixture had positive effect on the produced electricity. Azad [20] carried out an experimental analysis of thermal performance of solar collectors with different numbers of heat pipes. Li and Sun [21] carried out an operational performance study on a solar system. Jouhara et al. [22] reviewed heat pipe-based systems and pointed to the high efficiency of heat pipes as a passive heat transfer technology as the reason for their significant popularity. They also investigated the performance of a heat pipe-based solar system in district heating applications [23]. Long et al. [24] studied the application of the building integrated heat pipe systems in Hong Kong. He et al. [25] performed a theoretical investigation of the thermal performance of a novel LHP-based heat pump water heating system. Zhang et al. [26] scrutinized the characteristics of a solar system. They indicated that lower SRI, lower air temperature, higher air velocity, and smaller cover numbers brought about enhanced electrical efficiency while reducing thermal efficiency for the system. Chaudhry et al. [27] reviewed heat pipe systems for heat recovery and renewable energy applications. Maydanik [28] reviewed LHPs and suggested that LHPs were highly efficient heat transfer devices capable of transferring considerable heat flows over great distances.

The amount of solar radiation reaching the earth's surface varies depending on the geographic location, time of day, season, local landscape, and local weather [29]. The world has direct normal irradiation levels of 41.67–416.7 W/m^2 per day [30]. Thus, solar power can be harnessed using LHP-based solar systems. Although LHPs are simple and efficient heat transfer devices used in energy-efficient systems, no studies, according to the literature, have been conducted on the thermodynamic analysis of LHP-based energy systems.

In this study, a novel SCCHP system equipped with Solar Loop Heat Pipe Evaportor (SLHPE), an auxiliary pump, an absorption chiller, two evaporators, two storage tanks, a storage pump, a Storage Heat Exchanger (STHEX), a Regenerative Organic Rankine Cycle (RORC) turbine, an electrical generator, a Heating Process Heat Exchanger (HPHEX), a regenerator, a Domestic Water Heater (DWH), a Domestic Water Preheater (DWPH), and a RORC pump were thermodynamically modeled and assessed through energy and exergy analyses in three operation modes. In particular, the above-mentioned model was applied and tested in Tabriz, Iran. The main objectives of the present study are to better understand the functionality of the proposed system and propose a new, efficient, and sustainable solar thermal system. To this end, the following steps were taken into account:

- Model and simulate the SCCHP system;
- Validate each part of the model and simulation;
- Perform energy and exergy analyses of the SCCHP system;
- Perform a parametric study to determine the effect of major design parameters on the SCCHP system performance.

The main novelties of the present study lie in its analysis of the performance of a forced circulation SLHPS in a solar trigeneration system, utilization of new collector designs under real operational conditions, and consideration of a new way to incorporate the LHP operation principle into an SLHPS.

2. Material and methods

In this section, the specifications of the SCCHP system and its components for three operation modes are introduced.

2.1. System description

Figure 1 indicates the schematics of the proposed system.

The SCCHP system uses solar energy to evaporate working fluid (toluene in this study with the thermodynamic properties listed in Table 2) through the SLHPE, which drives the RORC evaporator, and vaporize the working fluid (n-hexane in this study with the thermodynamic properties listed in Table 2).

After leaving the RORC evaporator, n-hexane superheated vapor enters the turbine and following its passage through the turbine, the waste heat from the RORC is employed to produce process hot water and cooling and consequently, it passes through the DWH

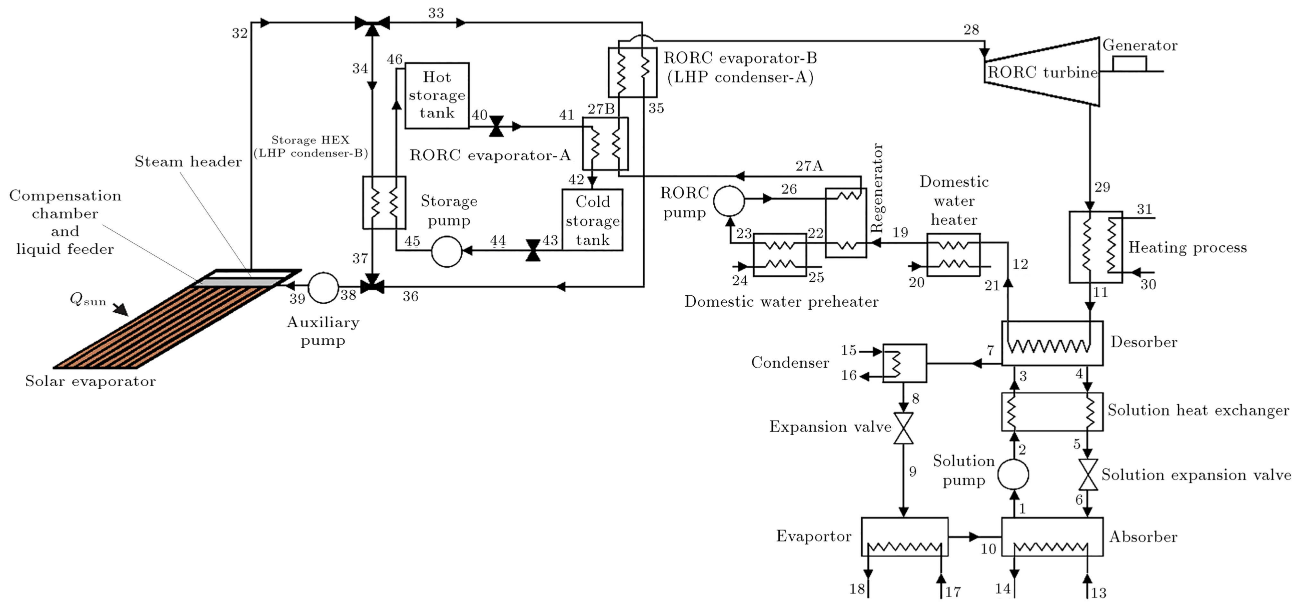

Figure 1. The schematic of the Solar Combined Cooling, Heating, and Power (SCCHP) system.

Table 2. Properties of working fluids for the Solar Combined Cooling, Heating, and Power (SCCHP) system.

Properties of toluene (working fluid for the SLHPS)		Properties of *n*-hexane (working fluid for the RORC)	
Parameter	**Value**	**Parameter**	**Value**
Chemical formula	C_7H_8	Chemical formula	C_6H_{14}
Molar mass (kg/kmol)	92.14	Molar mass (kg/kmol)	86.18
Boiling temperature (°C)	111	Boiling temperature (°C)	68.5 to 69.1
Density (kg/m^3)	867	Density (kg/m^3)	655
Freezing temperature (°C)	–95	Freezing temperature (°C)	–96 to –94
Critical temperature (°C)	318.6	Critical temperature (°C)	234.7
Critical pressure (MPa)	4.126	Critical pressure (MPa)	3.058

to produce domestic water. Since the working fluid has not reached the two phase states yet, at the outlet of the DWH, it is used to preheat the liquid before entering the RORC evaporator. The vapor is then condensed in the DWPH for warm water production. The working fluid is pumped into the regenerator and upon absorbing the heat, it streams to the RORC evaporator and the cycle is continuously repeated.

The SCCHP system comprises an SLHPE (including LHPs), a thermal sensor, vapor and liquid lines, vapor and liquid headers, compensation chamber, and RORC evaporator. In operation, the received solar energy transforms the toluene on the LHPs into saturated vapor, which streams along the LHPs to the vapor header mainly due to the buoyancy of vapor, auxiliary pump pressure, and gravity force created by the height difference between the RORC evaporator and SLHPE, as shown at Points 35 and 36 in Figure 1. The vapor is directed to the RORC evaporator through the vapor line. Then, through the liquid line, the toluene liquid enters the auxiliary pump. The auxiliary pump increases the pressure of the SLHPS working fluid and pumps it into the compensation chamber, which is placed under the vapor header. This amount of liquid is then divided and supplied to all of the LHP evaporators through a liquid feeder fixed at the upper part of the SLHPE, as shown in Figure 1. Furthermore, the liquid feeder pushes the liquid to descend into the LHP wicks equally. The schematic of LHP is shown in Figure 2.

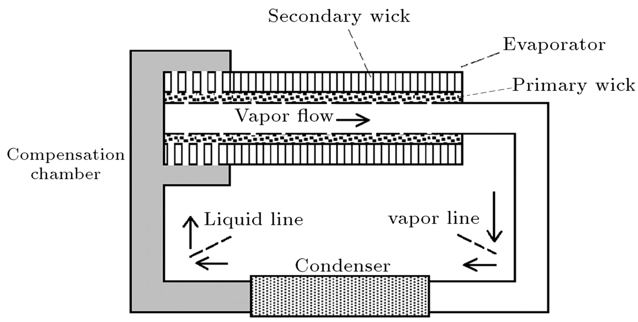

Figure 2. The schematic of Loop Heat Pipe (LHP).

Figure 3 shows the LHP as well as use of a three-path structure to supply rapid liquid distribution in the LHP wick.

Since the SRI varies with time, the SCCHP system in this study is supposed to work in three modes: solar mode (7:00 am to 9:00 am and 17:00 pm to 19:00 pm), solar and storage mode (9:00 am to 17:00 pm), and storage mode (19:00 pm to 7:00 am). Of note, 60% of the solar energy provided at the interval of 9:00 am to 17:00 pm is stored in the thermal storage tank. These modes are opted based on the average variations in the Solar Radiation Density (SRD) in the daytime in Tabriz, Iran. Figure 4 shows the average SRD variations in Tabriz, Iran and the three modes of operation for the SCCHP system, as well.

To conduct the thermodynamic analysis of the SCCHP, the following assumptions are taken into account:

- All the processes are considered to be operating in a steady state;
- Heat losses from piping and other components are neglected;
- There is an axisymmetric stream in all parts of the SLHPS;
- All of the SLHPS components are adiabatic except LHP evaporators;

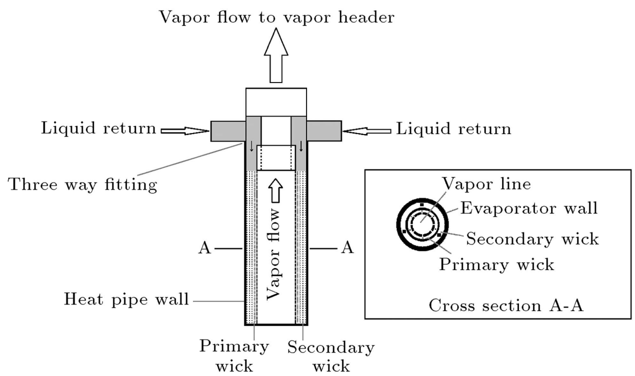

Figure 3. The schematic of three-way feeding and vapor/liquid separation structure.

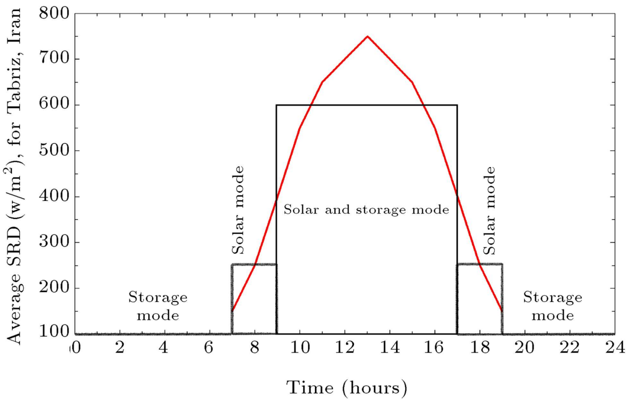

Figure 4. The average change of the Solar Radiation Density (SRD) in Tabriz, Iran, and three modes of operation for the Solar Combined Cooling, Heating, and Power (SCCHP) system.

- Pressure drops in the RORC cycle and absorption chiller are neglected;
- The dead states include $P_0 = 101$ kPa and $T_0 = 298.15$ K;
- The ambient temperature is $T_{amb} = 301.15$ K;
- The average solar radiations from 7:00 to 9:00 and 17:00 to 19:00 was 250 W/m^2, and from 9:00 to 17:00 was 600 W/m^2;
- Chemical exergy of components and the potential kinetic energy and exergy were not taken into consideration.

3. Analysis

For thermodynamic modeling of the SCCHP, the developed equations were programmed using EES software. The input data used in this model are given in Tables 3 and 4. The gravity effect pressure caused by the height difference between the RORC evaporator and SLHPE was +14.936 kPa (obtained using hydrostatic pressure equation), considered in the thermodynamic modeling of the SCCHP system.

In the forced circulation SLHPS, the system heat transfer capacity was controlled by five limits. According to Ref. [31], the heat transfer limits of the SLHPS are shown in Table 5.

The governing equations for the SCCHP are shown in Table 6. To model the SLHPS, the method used by Duffie and Beckman [32]was considered.

4. Result and discussion

In this section, the results of the thermodynamic modeling of the SCCHP system are presented.

4.1. Validation of the solar evaporator model

The SLHPE model was validated against the experimental study by Azad [33], as shown in Figure 5. The proposed model is in good agreement with the experimental work.

4.2. Validation of the CCHP cycle model

Since no theoretical and experimental study has been conducted in the field of the SLHPE-based CCHP sys-

Table 3. Input data for the Solar Combined Cooling, Heating, and Power (SCCHP) system.

Turbine efficiency	85%	Working fluid	n-hexane
Pumps efficiency	85%	Evaporator pinch point temperature, (°C)	2
HPHEX pinch point temperature (°C)	2	DWPH pinch point temperature, (°C)	2
DWPH pinch point temperature (°C)	4	HPHEX type	Plate heat exchanger
RORC pump inlet pressure (kPa)	20	RORC evaporator type	Plate heat exchanger
RORC turbine inlet pressure (kPa)	350	DWPH type	Plate heat exchanger
RORC turbine inlet temperature (°C)	119.7	DWH type	Plate heat exchanger
Generator inlet temperature range, T_{11} (°C)	55–60	Cooling cycle working fluid	LiBr water
Chilled water inlet temperature, T_{17} (°C)	10	Cooling water inlet temperature, T_{13} (°C)	25
Generator inlet mass flow rate, $\dot{m}_{11}$ (kg/sec)	0.41	Cooling water mass flow rate, $\dot{m}_{13}$ (kg/sec)	0.28
Solution pump mass flow rate, $\dot{m}_1$ (kg/sec)	0.05	Chilled water mass flow rate, $\dot{m}_{17}$ (kg/sec)	0.4
Cooling water mass flow rate to condenser, $\dot{m}_{15}$ (kg/sec)	0.28	Effectiveness of the solution heat exchanger	70%
Overall heat transfer coefficient of the absorber (kW/K)	1.8	Overall heat transfer coefficient of the evaporator (kW/K)	2.25
Overall heat transfer coefficient of the condenser (kW/K)	1.2	Overall heat transfer coefficient of the desorber (kW/K)	1

Table 4. Input data for the Solar Loop Heat Pipe System (SLHPS).

SLHPE length (m)	1.5	LHPs evaporator length (m)	1.5
Overall heat loss coefficient from the SLHPE to ambient temperature (kW/m^2.K)	0.005	SLHPE liquid filling mass (kg)	4.568
Overall heat loss coefficient from the SLHPE working fluid to ambient (kW/m^2.K)	0.0045	Critical radius of bubble generation for toluene (m)	0.00000007
SLHPE heat removal factor	0.83	LHPs material	Black Nickel
SLHPE to HPHEX height difference	1	SLHPE optical efficiency	0.8736
SLHPS heat exchanger height (m)	2	SLHPS condensers length (m)	2
SLHPS operating temperature range	100–126 (°C)	LHPs mesh ratio	1:1
Hot storage tank temperature drop (°C)	5	Cold storage tank temperature drop (°C)	3
RORC evaporator operating pressure range (kPa)	0–4500	LHPs type	Mesh screen
Number of LHP layers	Two layers	LHPs porosity	0.64
STHEX pinch point temperature (°C)	2	Internal diameter of the LHPs (m)	0.049
Thickness of the LHP wicks (m)	0.0075	Number of wick pores	18
Thickness of the LHP secondary wicks (m)	0.005	SLHPS vapor header material	Black Nickel
Thickness of the LHP primary wicks (m)	0.0025	Effective diameter of the wick pores (m)	0.1111
External diameter of the LHP evaporators (m)	0.05	SLHPS liquid line thickness (m)	0.002
Internal diameter of the LHP vapor lines (m)	0.041	SLHPS vapor line length (m)	3
RORC evaporator conductivity W/m.K	16	SLHPS vapor and liquid lines material	Cast iron
Thermal conductivity of the evaporator wall (W/m.K)	91	SLHPS vapor line diameter (m)	0.6
Thermal conductivity of evaporator wick (W/m.K)	91	LHPs wall thickness (m)	0.001
RORC evaporator (SLHPS condenser) and liquid line pressure drops (kPa)	6	SLHPS liquid line diameter (m)	0.5
Solar evaporator and vapor line pressure drops (kPa)	11	SLHPS liquid line length (m)	4
SLHPS average stream speed (m/sec)	50	SLHPS vapor line thickness (m)	0.002
SLHPE transmission factor (τ)	0.91	SLHPE absorption factor (α)	0.96

Table 5. The operating limits of the Solar Loop Heat Pipe System (SLHPS).

Operating limits	**Entrainment limit $\dot{Q}_{EL}$ (kW)**	**Viscous limit $\dot{Q}_{VL}$ (kW)**	**Sonic limit $\dot{Q}_{SL}$ (kW)**	**Boiling limit $\dot{Q}_{BL}$ (kW)**	**Filled liquid mass limit $\dot{Q}_{FL}$ (kW)**
Solar mode	2594	51899	312451	1145000	1032
Solar and storage mode	2657	53151	319994	1172000	1032

tems, the analysis of the SCCHP system was validated by the data provided by the Office of Energy Efficiency and Renewable Energy, Department of Energy, United States [34], as shown in Table 7, and the results were in good agreement.

4.3. Validation of the absorption chiller model

The analysis of the absorption chiller was validated by Herold et al. [35], as shown in Figure 6. According to this figure, considerable agreement between the current absorption chiller model and that of Herold et al. was observed.

4.4. Energy and exergy analysis results

The total numbers of the LHPs required by the SLHPE for the solar mode as well as the solar and storage mode were 6793 and 6957, respectively. The results obtained from the energy analysis of the SCCHP system are summarized in Table 8. In addition, the results of the exergy analysis of the SCCHP system are summarized in Table 9, suggesting that for both solar and solar and

Table 6. The governing equations for the Solar Combined Cooling, Heating, and Power (SCCHP) system.

SLHPS	$\dot{Q}_u = \dot{m}_{32}(h_{32} - h_{39})$ $\dot{Q}_u = A_{SOL,EVA} F_R (S - U_l(T_{39} - T_{amb}))$ $A_{SOL,EVA} = 0.75 N_{LHP} \pi D_o L_e$ $F_R = 0.83$ $S = \eta_{LHP} G_b$ $\eta_{LHP} = \tau\alpha$ $\eta_{en,SOL,EVA} = \frac{\dot{Q}_u}{G_b A_{SOL,EVA}}$ $\dot{E}_{SUN} = G_b A_{SOL,EVA} \left(1 + \frac{1}{3}\left(\frac{T_{amb}}{T_{SUN}}\right)^4 - \frac{4}{3}\left(\frac{T_{amb}}{T_{SUN}}\right)\right)$ $T_{SUN} = 4500$ K $\dot{I}_{SOL,EVA} = \dot{E}_{39} - \dot{E}_{32} + \dot{E}_{SUN}$
Auxiliary pump (solar mode)	$\dot{W}_{AUX,P} = \dot{m}_{39}(h_{39} - h_{38})$ $\dot{I}_{AUX,P} = \dot{E}_{38} + \dot{W}_{AUX,P} - \dot{E}_{39}$
RORC evaporator (evaporator B)	$\dot{m}_{33}(h_{33} - h_{35}) = \dot{m}_{27}(h_{28} - h_{27})$ $\dot{I}_{RORC,EVA} = \dot{E}_{33} + \dot{E}_{27} - \dot{E}_{28} - \dot{E}_{35}$
Auxiliary pump (solar and storage mode)	$\dot{m}_{38} = \dot{m}_{36} + \dot{m}_{37}$ $\dot{W}_{AUX,P} = \dot{m}_{39}(h_{39} - h_{38})$ $\dot{m}_{38} h_{38} = \dot{m}_{36} h_{36} + \dot{m}_{37} h_{37}$ $\dot{I}_{AUX,P} = \dot{E}_{38} + \dot{W}_{AUX,P} - \dot{E}_{39}$
STHEX	$\dot{m}_{34} = \frac{3}{2}\dot{m}_{33}$ $\dot{m}_{34} = \dot{m}_{32} - \dot{m}_{33}$ $\dot{m}_{34} = \dot{m}_{45}$ $\dot{m}_{46} = \dot{m}_{45}$ $\dot{m}_{34}(h_{34} - h_{37}) = \dot{m}_{45}(h_{46} - h_{45})$ $\dot{I}_{STHEX} = \dot{E}_{34} + \dot{E}_{45} - \dot{E}_{46} - \dot{E}_{37}$
Hot storage tank	$\dot{m}_{40} t_{CH,CST} = \dot{m}_{46} t_{CH,HST}$ $\dot{I}_{HST} = \dot{E}_{46} - \dot{E}_{40}$ $T_{40} = T_{46} - 5$ (HST temperature drop)
Hot storage tank valve	$\dot{m}_{41} = \dot{m}_{40}$ $h_{41} = h_{40}$ $\dot{E}_{41} = \dot{E}_{40}$
Cold storage tank	$\dot{m}_{42} t_{CH,CST} = \dot{m}_{43} t_{CH,HST}$ $\dot{I}_{CST} = \dot{E}_{42} - \dot{E}_{43}$ $T_{43} = T_{42} - 3$ (CST temperature drop)
Cold storage tank valve	$\dot{m}_{44} = \dot{m}_{43}$ $h_{44} = h_{43}$ $\dot{E}_{44} = \dot{E}_{43}$
Storage pump	$\dot{W}_{ST,P} = \dot{m}_{45}(h_{45} - h_{44})$ $\dot{I}_{ST,P} = \dot{E}_{44} + \dot{W}_{ST,P} - \dot{E}_{45}$

Table 6. The governing equations for the Solar Combined Cooling, Heating, and Power (SCCHP) system (continued).

RORC evaporator (evaporator A)	$\dot{m}_{41}(h_{41}-h_{42})=\dot{m}_{27}(h_{28}-h_{27})$ $\dot{I}_{RORC,EVA}=\dot{E}_{41}+\dot{E}_{27}-\dot{E}_{28}-\dot{E}_{42}$
RORC turbine	$\dot{W}_{RORC,T}=\dot{m}_{28}(h_{28}-h_{29})$ $\dot{I}_{RORC,T}=\dot{E}_{28}-\dot{E}_{29}-\dot{W}_{RORC,T}$
Process heat exchanger	$\dot{m}_{29}(h_{29}-h_{11})=\dot{m}_{HP}(h_{31}-h_{30})$ $\dot{I}_{HP}=\dot{E}_{29}+\dot{E}_{30}-\dot{E}_{11}-\dot{E}_{31}$
Regenerator	$\dot{m}_{19}(h_{19}-h_{22})=\dot{m}_{26}(h_{27}-h_{26})$ $\dot{I}_{REG}=\dot{E}_{19}+\dot{E}_{26}-\dot{E}_{22}-\dot{E}_{27}$
DWPH	$\dot{m}_{22}(h_{22}-h_{23})=\dot{m}_{DWPH}(h_{25}-h_{24})$ $\dot{I}_{DWPH}=\dot{E}_{22}+\dot{E}_{24}-\dot{E}_{23}-\dot{E}_{25}$
DWH	$\dot{m}_{12}(h_{12}-h_{19})=\dot{m}_{DWH}(h_{21}-h_{20})$ $\dot{I}_{DWH}=\dot{E}_{12}+\dot{E}_{20}-\dot{E}_{19}-\dot{E}_{21}$
RORC pump	$\dot{W}_{RORC,P}=\dot{m}_{26}(h_{26}-h_{23})$ $\dot{I}_{RORC,P}=\dot{E}_{23}-\dot{E}_{26}+\dot{W}_{RORC,P}$
Absorber	$\dot{m}_{10}=\dot{m}_6+\dot{m}_1$ $\dot{m}_1x_1=\dot{m}_6x_6$ $\dot{m}_{10}h_{10}+\dot{m}_6h_6=\dot{m}_1h_1+\dot{Q}_{ABS}$ $\dot{I}_{ABS}=\dot{E}_{10}+\dot{E}_6+\dot{E}_{13}-\dot{E}_1-\dot{E}_{14}$
Solution pump	$\dot{W}_{SP}=\dot{m}_2(h_2-h_1)$ $\dot{I}_{SP}=\dot{E}_1-\dot{E}_2+\dot{W}_{SP}$
Solution heat exchanger	$\dot{m}_2=\dot{m}_3$ $\dot{m}_4=\dot{m}_5$ $x_2=x_3$ $x_4=x_5$ $\dot{m}_2h_2+\dot{m}_4h_4=\dot{m}_3h_3+\dot{m}_5h_5$ $\dot{I}_{SHEX}=\dot{E}_2+\dot{E}_4-\dot{E}_3-\dot{E}_5$
Desorber	$\dot{m}_3=\dot{m}_4+\dot{m}_7$ $\dot{m}_4x_4=\dot{m}_3x_3$ $\dot{m}_{11}(h_{11}-h_{12})+\dot{m}_3h_3=\dot{m}_7h_7+\dot{m}_4h_4$ $\dot{I}_{GEN}=\dot{E}_{11}+\dot{E}_3-\dot{E}_4-\dot{E}_7-\dot{E}_{12}$
Expansion valves	$\dot{m}_9=\dot{m}_8$ $\dot{m}_6=\dot{m}_5$ $h_9=h_8$ $h_6=h_5$ $\dot{I}_{EXV}=\dot{E}_8+\dot{E}_5-\dot{E}_9-\dot{E}_6$

Table 6. The governing equations for the Solar Combined Cooling, Heating, and Power (SCCHP) system (continued).

Condenser	$\dot{m}_8 = \dot{m}_7$ $\dot{m}_7 h_7 = \dot{m}_8 h_8 + \dot{Q}_{Cond}$ $\dot{I}_{Cond} = \dot{E}_7 + \dot{E}_{15} - \dot{E}_8 - \dot{E}_{16}$
Evaporator	$\dot{m}_9 = \dot{m}_{10}$ $\dot{Q}_{EVP} = \dot{m}_{10} h_{10} - \dot{m}_9 h_9$ $\dot{I}_{EVP} = \dot{E}_{17} + \dot{E}_9 - \dot{E}_{18} - \dot{E}_{10}$
The log mean temperature difference method formulas	$\dot{Q} = UA.LMTD$ $LMTD = \frac{(T_{h,in}-T_{c,out})-(T_{h,out}-T_{c,in})}{\ln\left[\frac{T_{h,in}-T_{c,out}}{T_{h,out}-T_{c,in}}\right]}$
The energy efficiency of the SCCHP system for the solar mode	$\eta_{en} = \frac{\dot{Q}_{HP}+\dot{Q}_{DWH}+\dot{Q}_{DWPH}+\dot{Q}_{EVP}+\dot{W}_{Net,T}}{G_b A_{SOL,EVA}}$
The exergy efficiency of the SCCHP system for the solar mode	$\eta_{ex} = \frac{\dot{W}_{Net,T}+\dot{E}_{DWPH,out}-\dot{E}_{DWPH,in}+\dot{E}_{DWH,out}-\dot{E}_{DWH,in}+\dot{E}_{HP,out}-\dot{E}_{HP,in}+\dot{E}_{18}-\dot{E}_{17}}{\dot{E}_{SUN}}$
The energy efficiency of the SCCHP system for the solar and storage mode	$\eta_{en} = \frac{\dot{Q}_{ST,HEX}+\dot{Q}_{HP}+\dot{Q}_{DWH}+\dot{Q}_{DWPH}+\dot{Q}_{EVP}+\dot{W}_{Net,T}}{G_b A_{SOL,EVA}}$
The exergy efficiency of the SCCHP system for the solar and storage mode	$\eta_{ex} = \frac{\dot{W}_{Net,T}+\dot{E}_{DWPH,out}-\dot{E}_{DWPH,in}+\dot{E}_{DWH,out}-\dot{E}_{DWH,in}+\dot{E}_{HP,out}-\dot{E}_{HP,in}+\dot{E}_{18}-\dot{E}_{17}+\dot{E}_{46}-\dot{E}_{45}}{\dot{E}_{SUN}}$
The energy efficiency of the SCCHP system for the storage mode	$\eta_{en} = \frac{\dot{Q}_{HP}+\dot{Q}_{DWH}+\dot{Q}_{DWPH}+\dot{Q}_{EVP}+\dot{W}_{Net,T}}{\dot{m}_{34}(h_{34}-h_{37})}$
The exergy efficiency of the SCCHP system for the storage mode	$\eta_{ex} = \frac{\dot{W}_{Net,T}+\dot{E}_{DWPH,out}-\dot{E}_{DWPH,in}+\dot{E}_{DWH,out}-\dot{E}_{DWH,in}+\dot{E}_{HP,out}-\dot{E}_{HP,in}+\dot{E}_{18}-\dot{E}_{17}}{\dot{E}_{34}-\dot{E}_{37}}$

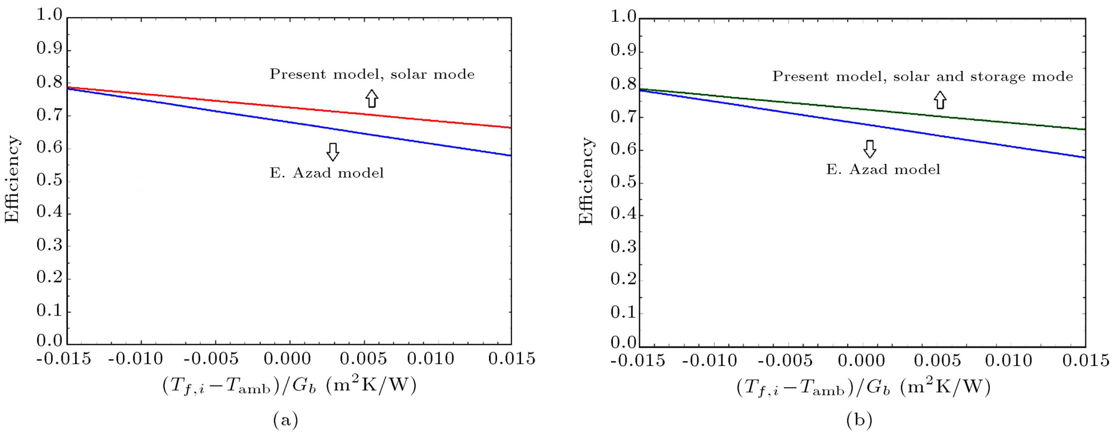

Figure 5. Validation of the Solar Loop Heat Pipe Evaportor (SLHPE) model in comparison with Azad's model [33]: (a) solar mode and (b) solar and storage mode.

Table 7. Validation of the Solar Combined Cooling, Heating, and Power (SCCHP) cycle model.

Data from United States Department of Energy	Present study (solar mode)	Present study (solar and storage mode)
Reasonable efficiency of overall CCHP cycle: 65–75%	Overall CCHP cycle efficiency: 70.52%	Overall CCHP cycle efficiency: 72.09%

Table 8. The results of the energy analysis of the Solar Combined Cooling, Heating, and Power (SCCHP) system.

Parameter	Solar mode	Solar and storage mode	Storage mode
SLHPE useful energy	212.7 kW	532.9 kW	—
HPHEX energy flow	8.108 kW	8.108 kW	4.438 kW
DWH energy flow	19.04 kW	19.04 kW	19.04 kW
DWPH energy flow	148.3 kW	148.3 kW	148.3 kW
Regenerator energy flow	2.062 kW	2.062 kW	2.062 kW
RORC evaporator energy flow	212.7 kW	212.7 kW	208.6 kW
RORC turbine net power	33.2 kW	33.19 kW	32.58 kW
RORC pump input power	0.2414 kW	0.2414 kW	0.2414 kW
Auxiliary pump input power	0.001131 kW	0.008945 kW	—
Desorber energy flow	4.134 kW	4.134 kW	4.134 kW
Condenser energy flow	3.111 kW	3.111 kW	3.111 kW
Evaporator energy flow	3.008 kW	3.008 kW	3.008 kW
Absorber energy flow	4.031 kW	4.031 kW	4.031 kW
Solution pump input power	0.00009977 kW	0.00009977 kW	0.00009977 kW
STHEX energy flow	—	320.1 kW	320.1 kW
Storage pump input power	—	—	0.09917 kW
SCCHP cycle efficiency	70.52%	72.09%	64.77%

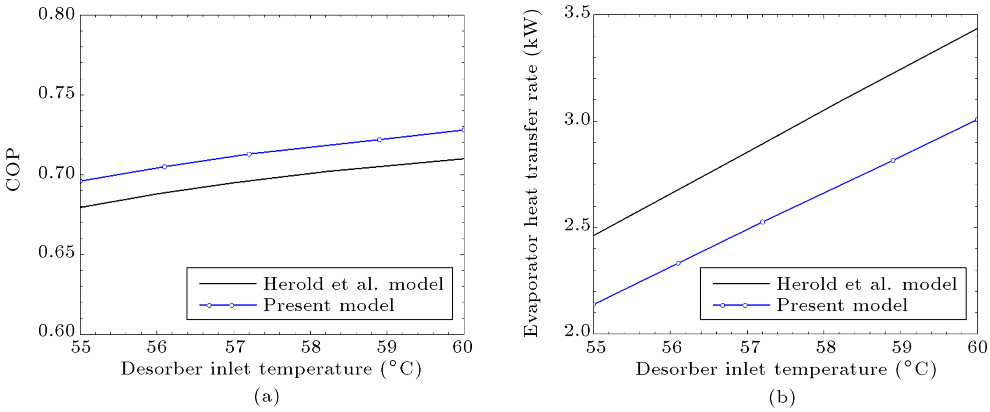

Figure 6. Validation of the absorption chiller model against the model proposed by Herold et al., Coefficient of Performance (COP), and evaporator heat rate versus generator inlet temperature.

storage modes, the main source of exergy destruction is the SLHPE, while for the storage mode, the main source of exergy destruction is the hot storage tank.

4.5. The effect of variations of the RORC evaporator pinch point temperature on the SCCHP cycle performance

Figure 7 shows the RORC evaporator pinch point temperature variations with the energy and exergy efficiencies, SCCHP cycle exergy destruction rate, heat flow of the RORC evaporator, and turbine work for the three operation modes. As the pinch point temperature increased, the heat absorbed by the RORC evaporator decreased and the utilization of this energy decreased. Therefore, the enthalpy of the n-hexane vapor in the RORC evaporator decreased which reduced the RORC evaporator heat flow and increased the overall cycle exergy destruction rate, leading to a decrease in the energy and exergy efficiency of the proposed system for all three operating modes.

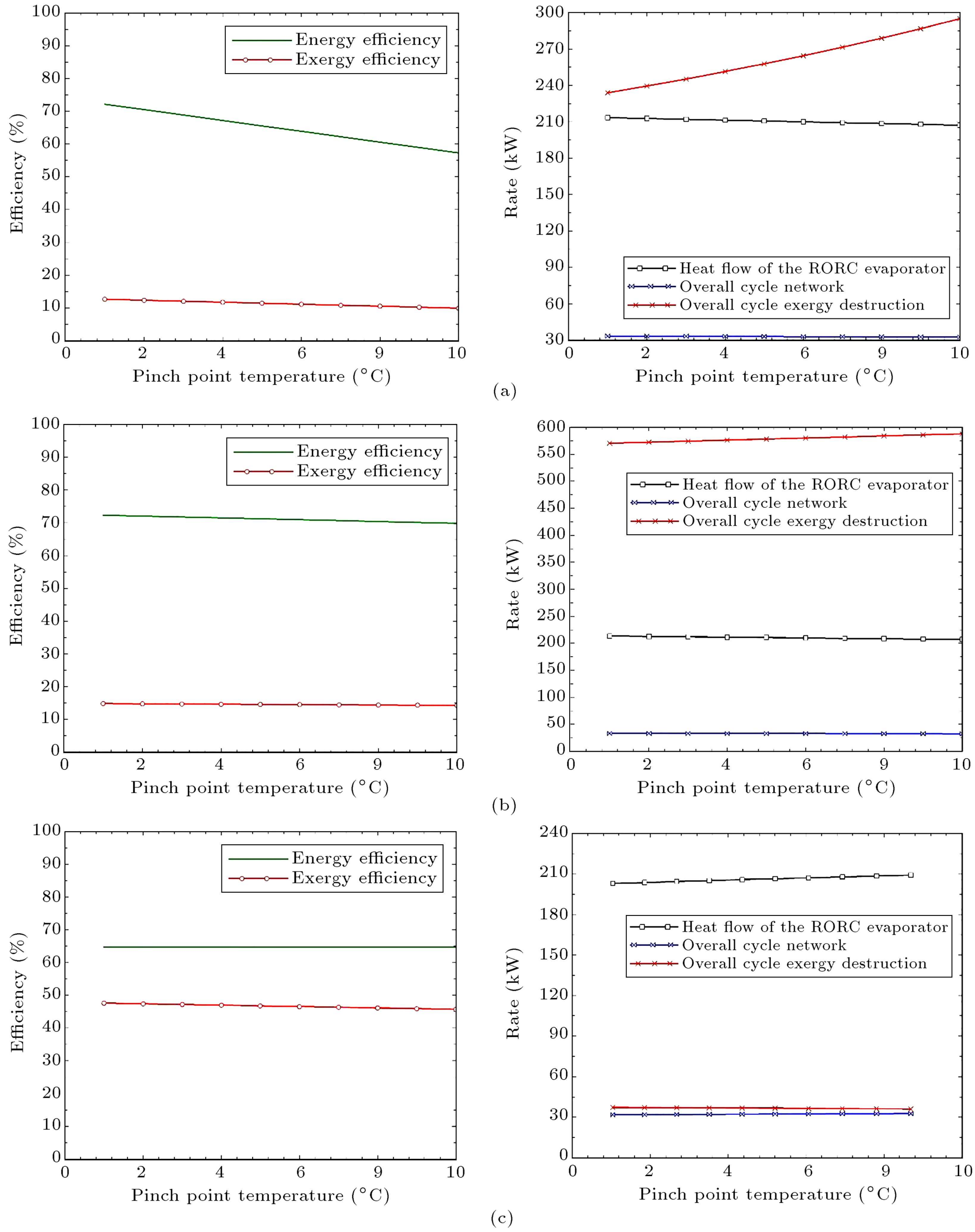

Figure 7. Variation in the Regenerative Organic Rankine Cycle (RORC) evaporator pinch point temperature with the energy efficiency, exergy efficiency, overall cycle exergy destruction rate, heat flow of the RORC evaporator, and the turbine work: (a) Solar mode, (b) solar and storage mode, and (c) storage mode.

4.6. The effect of varying ambient temperature on the SCCHP cycle performance

Figure 8 shows the variation of energy and exergy efficiencies as well as the SLHPE exergy destruction rate with ambient temperature in both solar and solar and storage modes. As observed earlier, increasing the ambient temperature would increase the energy and exergy efficiencies of the SCCHP system, decrease the SLHPE exergy destruction rate, mainly because the SLHPS was designed to produce toluene saturated vapor, decrease the SLHPE heat losses and the total number of the LHPs, and finally reduce the SLHPE exergy destruction rate for the solar and the solar and storage modes.

4.7. The effect of variations in the SRI on the SCCHP cycle performance

Figure 9 shows the variations in energy and exergy efficiencies and solar evaporator exergy destruction rate with SRI for both solar and the solar and storage

Table 9. The results of the exergy analysis of the Solar Combined Cooling, Heating, and Power (SCCHP) system.

Parameter	Solar mode	Solar and storage mode	Storage mode
SLHPE exergy destruction rate	227.4 kW	557 kW	—
RORC evaporator exergy destruction rate	5.336 kW	5.336 kW	3.228 kW
RORC turbine exergy destruction rate	5.175 kW	5.175 kW	5.168 kW
DWPH exergy destruction rate	1.258 kW	1.258 kW	1.258 kW
DWH exergy destruction rate	1.293 kW	0.09601 kW	0.09601 kW
STHEX exergy destruction rate	—	3.351 kW	3.351 kW
Hot storage tank exergy destruction rate	—	—	22.77 kW
Cold storage tank exergy destruction rate	—	—	0.03913 kW
Other components exergy destruction rate	1.465 kW	1.43079 kW	1.5048 kW
SCCHP cycle efficiency	12.36%	14.78%	47.45%

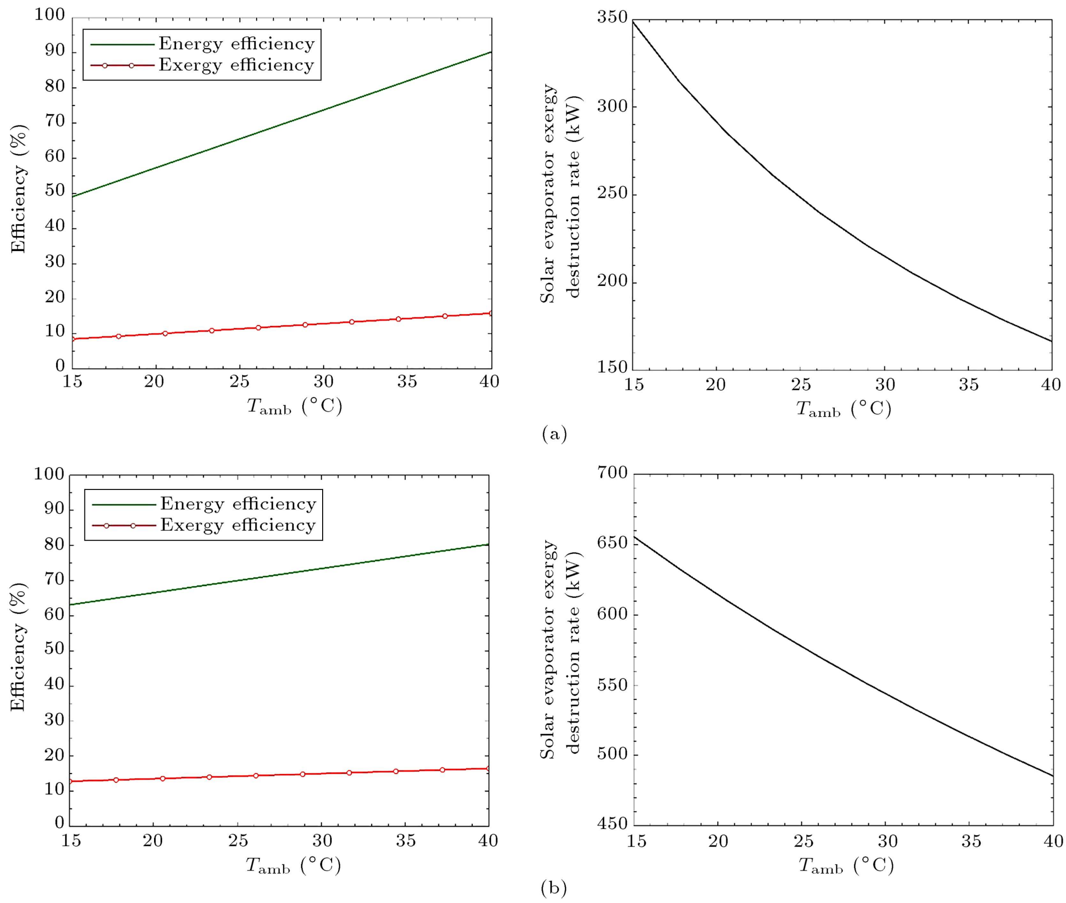

Figure 8. Variation in the ambient temperature with the energy efficiency, exergy efficiency, and solar evaporator exergy destruction rate for (a) solar mode and (b) solar and storage mode.

modes. As observed earlier, increasing the SRI would increase the energy and exergy efficiencies of the proposed system due to an increase in the SRI, and decrease the solar evaporator heat losses and exergy destruction rate for the solar and the solar and storage operation modes. These results were obtained because the SLHPS was designed to produce toluene saturated vapor; furthermore, increasing the SRI would reduce the SLHPE heat losses and the total number of the LHPs, decrease the SLHPE exergy destruction rate for both solar and the solar and storage modes, and improve the SCCHP cycle performance.

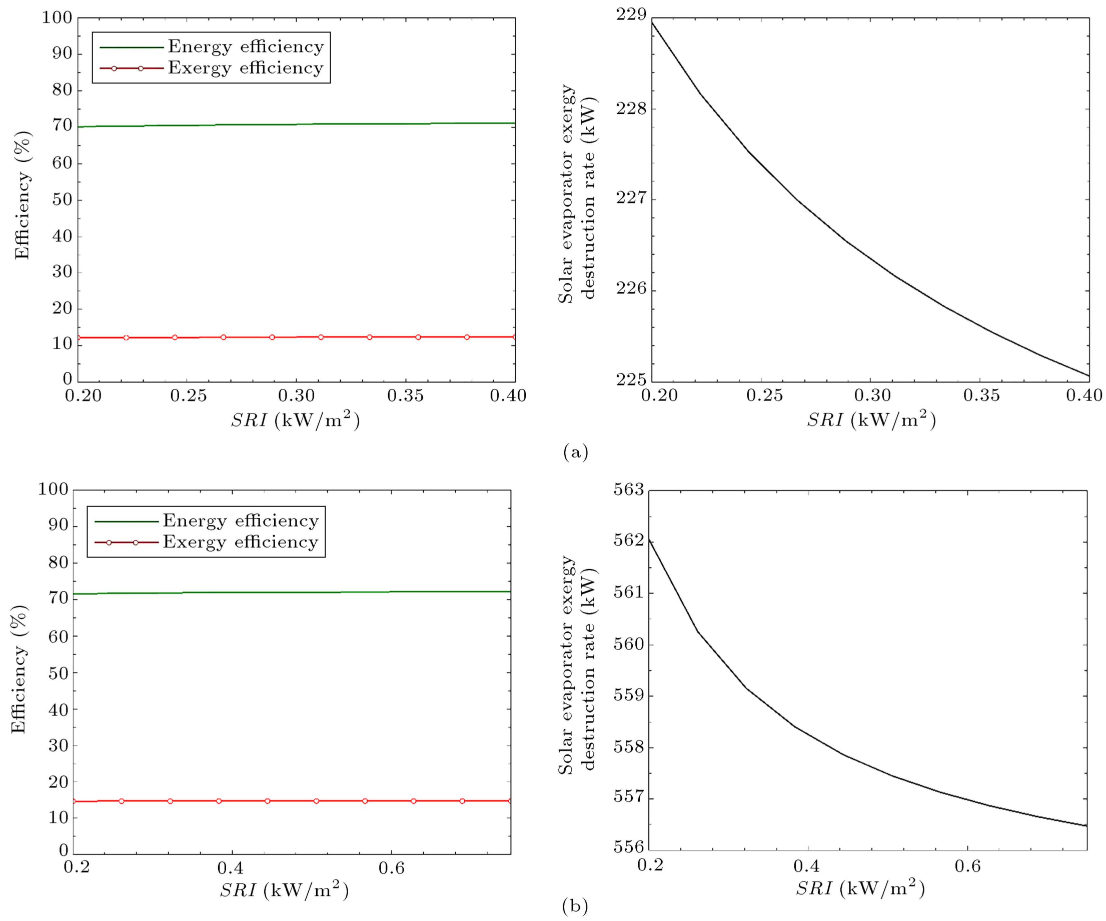

Figure 9. Variation in Solar Radiation Intensity (SRI) of the energy efficiency, exergy efficiency, and solar evaporator exergy destruction rate for (a) solar mode and (b) solar and storage mode.

4.8. The effect of variations in the turbine inlet pressure on the SCCHP cycle performance

Figure 10 shows the variations in energy and exergy efficiencies, turbine work rate, and overall cycle exergy destruction rate with turbine inlet pressure in all of the three operation modes. As observed earlier, with an increase in the turbine inlet pressure, the energy efficiency decreased and the turbine work rate increased. Moreover, such an increase in turbine inlet pressure led to a decrease in turbine extraction temperature; besides, since this temperature was the primary flow temperature for the HPHEX, a reduction in the primary enthalpy of the HPHEX, energy flow of the HPHEX, and heating load of the HPHEX was observed. Figure 10 shows that an increase in the turbine inlet pressure would enhance the exergy efficiency of the SCCHP system. As the turbine inlet pressure increased, the enthalpy drops across the turbine increased, the overall irreversibility of the SCCHP system decreased, and the net power output of the system increased. Moreover, small temperature differences between the fluid streams improved the exergy efficiency of the system in all of the three operation modes.

5. Conclusions

In this study, the steady state thermodynamic analysis of the Solar Combined Cooling, Heating, and Power (SCCHP) system in all of the three operation modes was conducted. The present study aimed to find, expand, and model a new loop-heat-pipe-based SCCHP system and introduce a sustainable and renewable novel solar system. The results showed that while the main source of the exergy destruction for both solar and the solar and storage modes was the SLHPE, it was the hot storage tank for the storage mode. The energy efficiency of the proposed system was 70.52% for the solar mode, 72.09% for the solar and storage mode, and 64.77% for the storage mode. In addition, the exergy efficiency of the proposed system was 12.36% for the solar mode, 14.78% for the solar and storage mode, and 47.45% for the storage mode. Loop Heat Pipes (LHPs) could significantly contribute to the development of solar thermal systems due to their potential for low-

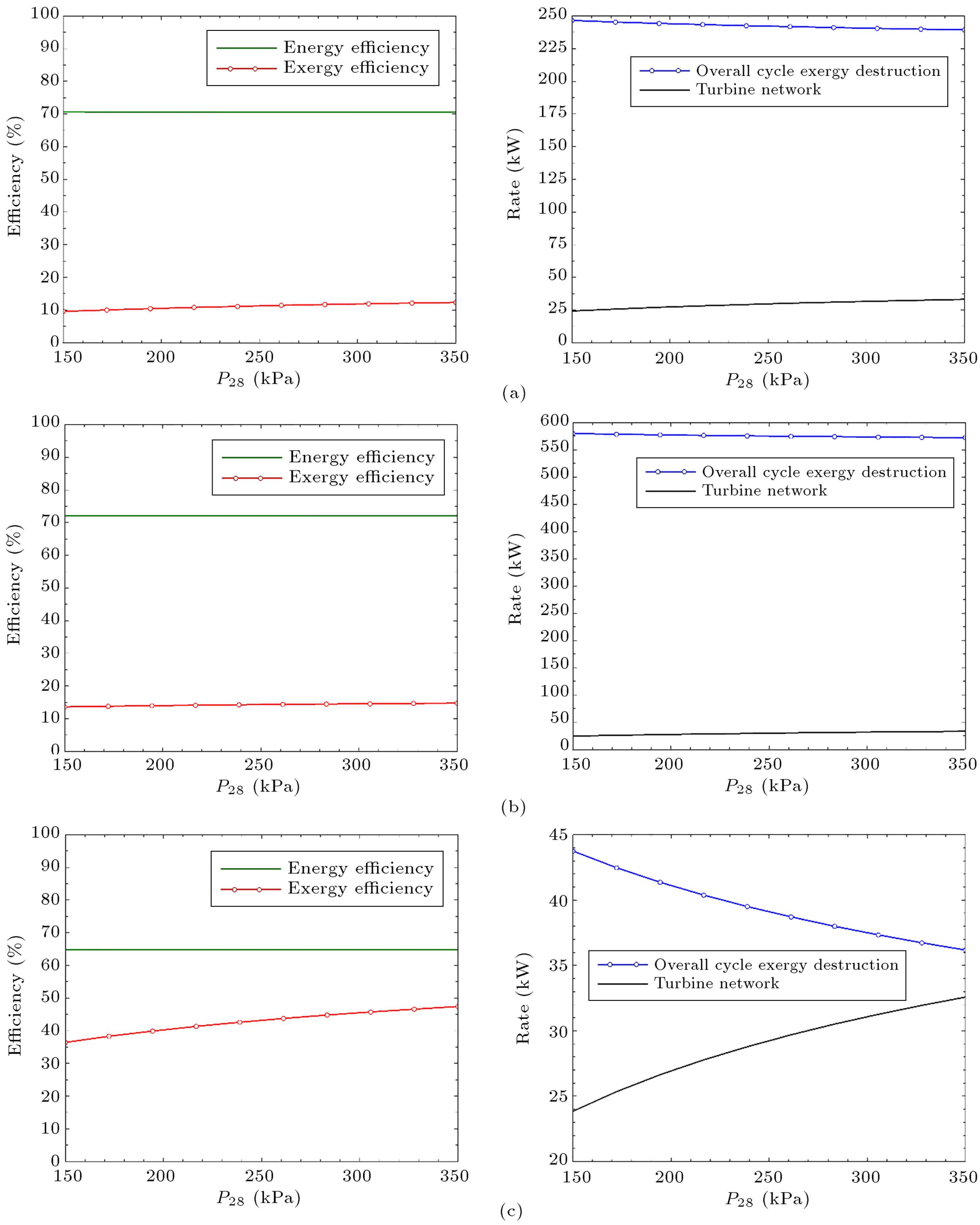

Figure 10. Variation in the turbine inlet pressure with the energy efficiency, exergy efficiency, turbine work rate, and overall cycle exergy destruction rate for (a) solar mode, (b) solar and storage mode, and (c) storage mode.

thermal resistance, high-thermal capacity, and simple structure. The results of this research facilitate a better understanding of the performance of SLHPEs and create new layouts associated with designing the LHP-based solar thermal systems.

Acknowledgements

The authors are thankful for the Management and Staff of National Iranian Oil Refining and Distribution Company for their technical support.

Nomenclature

A	Area (m^2)
cv	Control volume
CHP	Combined Heating and Power
CCHP	Combined Cooling, Heating, and Power
CSP	Concentrated Solar Power
COP	Coefficient Of Performance
D	Vapor line diameter

DWH	Domestic Water Heater
DWPH	Domestic Water Preheater
E	Energy
e	Exit
$\dot{E}$	Exergy rate (kW)
$\dot{E}_{\mathrm{SUN}}$	The total inlet exergy to the cycle (kW)
F_R	SLHPE heat removal factor
G_b	Solar radiation (W/m^2)
h	Specific enthalpy (kj/kg)
HPHEX	Heating Process Heat Exchanger
i	Inlet
$\dot{I}$	Exergy destruction rate (kW)
K	Kelvin
kWh	Kilowatt hour
kg	Kilograms
L	Length
LMTD	Log Mean Temperature Difference (°C)
L_e	Solar evaporator length
LHP	Loop Heat Pipe
m_f	Solar evaporator liquid filling mass (kg)
$\dot{m}$	Mass flow rate (kg/sec)
m	Mass or meter
N_P	Number of wick pores
N_{LHP}	Number of LHPs
out	Exit
P	Pressure (kPa)
Pa	Pascal
PV	Photovoltaic
PVT	Photovoltaic Thermal
PCM	Phase Change Material
$\dot{Q}$	Heat rate (kW)
RORC	Regenerative Organic Rankine Cycle
SRD	Solar Radiation Density
SOL, EVA	Solar loop heat pipe evaporator
s	Specific entropy (kj/kg.K)
sec	Second
SLHPS	Solar Loop Heat Pipe System
S	Radiation absorbed by the SLHPE
SRI	Solar Radiation Intensity
STHEX	Storage Heat Exchanger
SCCHP	Solar CCHP
SLHPE	Solar Loop Heat Pipe Evaporator
T	Temperature
T_{SUN}	Sun temperature (K)
t	Time
U_l	Overall heat loss coefficient from SLHPE to ambient, (kW/m^2.K)
U	Heat transfer coefficient (kW/m^2.K)
UA	Overall heat transfer coefficient (kW/K)
$\dot{W}_{Net,T}$	Turbine work rate (kW)
$\dot{W}$	Work rate (kW)
W	Watts
x	LiBr mass concentration

Greek symbols

α	The SLHPE absorption factor
δ	Thickness
η	Efficiency
η_{LHP}	LHP optical efficiency
τ	SLHPE transmission factor
ψ	Specific exergy (kJ/kg)

Subscripts

AUX, P	Auxiliary Pump
ABS	Absorber
amb	Ambient
BL	Boiling Limit
$Cond$	Condenser
CST	Cold Storage Tank
CH, HST	Charging time of the Hot Storage Tank
CH, CST	Charging time of the Cold Storage Tank
DWH	Domestic Water Heater
$DWPH$	Domestic water preheater
EXV	Expansion Valve
EVP	Evaporator
EL	Entrainment Limit
ex	Exergy efficiency
en	Energy efficiency
FL	Filled Liquid mass limit
f, i	Fluid entering solar evaporator
GEN	Generator (desorber)
$Heat$	Exergy transfer by heat (kW)
HP	Heating Process
HST	Hot Storage Tank
in	Inlet
o	Outer
out	Outlet
pw	LHPs primary wick

$RORC,T$	RORC Turbine
$RORC,P$	RORC Pump
$RORC,EVA$	RORC Evaporator
REG	Regenerator
SL	Sonic Limit
SP	Solution Pump
SUN	Sun
$SHEX$	Solution heat exchanger
sw	LHP secondary wick
SOL,EVA	Solar loop heat pipe evaporator
ST,P	Storage Pump
u	Useful
vh	Vapor header
VL	Viscous Limit
w	LHP wicks

References

1. Villarini, M., Tascioni, R., Arteconi, A., and Cioccolanti, L. "Influence of the incident radiation on the energy performance of two small-scale solar organic Rankine cycle trigenerative systems: A simulation analysis", *Applied Energy*, **242**, pp. 1176–1188 (2019).

2. Dabwan, Y.N., Pei, G., Gao, G., Li, J., and Feng, J. "Performance analysis of integrated linear fresnel reflector with a conventional cooling, heat, and power tri-generation plant", *Renewable Energy*, **138**, pp. 639–650 (2019).

3. Bellos, E. and Tzivanidis, C. "Evaluation of a solar driven trigeneration system with conventional and new criteria", *International Journal of Sustainable Energy*, **38**(3), pp. 238–252 (2019).

4. Bellos, E. and Tzivanidis, C. "Parametric analysis and optimization of a solar driven trigeneration system based on ORC and absorption heat pump", *Journal of Cleaner Production*, **161**, pp. 493–509 (2017).

5. Su, B., Han, W., and Jin, H. "Proposal and assessment of a novel integrated CCHP system with biogas steam reforming using solar energy", *Applied Energy*, **206**, pp. 1–11 (2017).

6. Corumlu, V., Ozsoy, A., and Ozturk, M. "Thermodynamic studies of a novel heat pipe evacuated tube solar collectors based integrated process for hydrogen production", *International Journal of Hydrogen Energy*, **43**(2), pp. 1060–1070 (2018).

7. Khan, J. and Arsalan, M.H. "Solar power technologies for sustainable electricity generation-A review", *Renewable and Sustainable Energy Reviews*, **55**, pp. 414–425 (2016).

8. Sampaio, P.G.V. and González, M.O.A. "Photovoltaic solar energy: Conceptual framework", *Renewable and Sustainable Energy Reviews*, **74**, pp. 590–601 (2017).

9. Maydanik, Y., Pastukhov, V., and Chernysheva, M. "Development and investigation of a loop heat pipe with a high heat-transfer capacity", *Applied Thermal Engineering*, **130**, pp. 1052–1061 (2018).

10. Yunus, A.C., *Heat Transfer a Practical Approach*, McGraw-Hill (2003).

11. Shafieian, A., Khiadani, M., and Nosrati, A. "Strategies to improve the thermal performance of heat pipe solar collectors in solar systems: A review", *Energy Conversion and Management*, **183**, pp. 307–331 (2019).

12. Shafieian, A., Khiadani, M., and Nosrati, A. "Thermal performance of an evacuated tube heat pipe solar water heating system in cold season", *Applied Thermal Engineering*, **149**, pp. 644–657 (2019).

13. Allouhi, A., Amine, M.B., Buker, M.S., Kousksou, T., and Jamil, A. "Forced-circulation solar water heating system using heat pipe-flat plate collectors: Energy and exergy analysis", *Energy*, **180**, pp. 429–443 (2019).

14. Li, H. and Sun, Y. "Performance optimization and benefit analyses of a photovoltaic loop heat pipe/solar assisted heat pump water heating system", *Renewable Energy*, **134**, pp. 1240–1247 (2019).

15. Diallo, T.M., Yu, M., Zhou, J., Zhao, X., Shittu, S., Li, G., Ji, J., and Hardy, D. "Energy performance analysis of a novel solar PVT loop heat pipe employing a microchannel heat pipe evaporator and a PCM triple heat exchanger", *Energy*, **167**, pp. 866–888 (2019).

16. Lu, Y. and Wang, J. "Thermodynamics performance analysis of solar-assisted combined cooling, heating and power system with thermal storage", *Energy Procedia*, **142**, pp. 3226–3233 (2017).

17. Hands, S., Sethuvenkatraman, S., Peristy, M., Rowe, D., and White, S. "Performance analysis & energy benefits of a desiccant based solar assisted trigeneration system in a building", *Renewable Energy*, **85**, pp. 865–879 (2016).

18. Wang, J., Lu, Y., Yang, Y., and Mao, T. "Thermodynamic performance analysis and optimization of a solar-assisted combined cooling, heating and power system", *Energy*, **115**, pp. 49–59 (2016).

19. Yuksel, Y.E., Ozturk, M., and Dincer, I. "Thermodynamic performance assessment of a novel environmentally-benign solar energy based integrated system", *Energy Conversion and Management*, **119**, pp. 109–120 (2016).

20. Azad, E. "Experimental analysis of thermal performance of solar collectors with different numbers of heat pipes versus a flow-through solar collector", *Renewable and Sustainable Energy Reviews*, **82**, pp. 4320–4325 (2018).

21. Li, H. and Sun, Y. "Operational performance study on a photovoltaic loop heat pipe/solar assisted heat pump water heating system", *Energy and Buildings*, **158**, pp. 861–872 (2018).

22. Jouhara, H., Chauhan, A., Nannou, T., Almahmoud, S., Delpech, B., and Wrobel, L.C. "Heat pipe based systems-Advances and applications", *Energy*, **128**, pp. 729–754 (2017).

23. Jouhara, H., Szulgowska-Zgrzywa, M., Sayegh, M.A., Milko, J., Danielewicz, J., Nannou, T.K., and Lester, S.P. "The performance of a heat pipe based solar PV/T roof collector and its potential contribution in district heating applications", *Energy*, **136**, pp. 117–125 (2017).

24. Long, H., Chow, T.T., and Ji, J. "Building-integrated heat pipe photovoltaic/thermal system for use in Hong Kong", *Solar Energy*, **155**, pp. 1084–1091 (2017).

25. He, W., Hong, X., Zhao, X., Zhang, X., Shen, J., and Ji, J. "Theoretical investigation of the thermal performance of a novel solar loop-heat-pipe facade-based heat pump water heating system", *Energy and Buildings*, **77**, pp. 180–191 (2014).

26. Zhang, X., Zhao, X., Xu, J., and Yu, X. "Characterization of a solar photovoltaic/loop-heat-pipe heat pump water heating system", *Applied Energy*, **102**, pp. 1229–1245 (2013).

27. Chaudhry, H.N., Hughes, B.R., and Ghani, S.A. "A review of heat pipe systems for heat recovery and renewable energy applications", *Renewable and Sustainable Energy Reviews*, **16**(4), pp. 2249–2259 (2012).

28. Maydanik, Y.F. "Loop heat pipes", *Applied Thermal Engineering*, **25**(5–6), pp. 635–657 (2005).

29. https://www.energy.gov/eere/solar/articles/solar-radiation-basics.

30. https://globalsolaratlas.info/downloads/world.

31. Chi, S.W., *Heat Pipe Theory and Practice: A Source Book*, Hemisphere Pub. Corp. (1976).

32. Duffie, J.A. and Beckman, W.A., *Solar Engineering of Thermal Processes*, John Wiley & Sons (2013).

33. Azad, E. "Assessment of three types of heat pipe solar collectors", *Renewable and Sustainable Energy Reviews*, **16**(5), pp. 2833–2838 (2012).

34. https://www.energy.gov/eere/amo/combined-heat-and-power-basics.

35. Herold, K.E., Radermacher, R., and Klein, S.A., *Absorption Chillers and Heat Pumps*, CRC press (2016).

36. Faghri, A., *Heat Pipe Science and Technology*, Global Digital Press (1995).

37. Cotter, T.P., *Theory of Heat Pipes (No. LA-3246)*, Los Alamos Scientific Lab., Univ. of California, N. Mex. (1965).

Appendix

Heat pipe theory

Heat transfer by heat pipes is one of the fastest and most efficient methods. Heat pipes are highly conductive heat transfer devices. They use the latent heat of the working fluids for efficient heat transfer. The operation of LHPs is based on the same physical processes as those used in conventional heat pipes. However, they are organized in quite a different way. For further details, please refer to [9,22,27,28,31,32,36,37].

Biographies

Vahid Beygzadeh received his BSc, MSc, and PhD degrees in Mechanical Engineering from the Urmia University (2010), Tabriz University (2012), and Urmia University of Technology (2018), respectively. His research interests include energy systems and heat transfer.

Shahram Khalilarya received his BSc, MSc, and PhD degrees in Mechanical Engineering from Tabriz University (1987), Tabriz University (1990), and Bath University (2001), respectively. He is currently an academic staff member at the Department of Mechanical Engineering at the Urmia University. His research interests include internal combustion engines and energy systems.

Iraj Mirzaee received his BSc, MSc, and PhD degrees in Mechanical Engineering from Ferdowsi University of Mashhad (1986), Isfahan University of Technology (1989), and Bath University (1997), respectively. He is currently an academic staff member at the Department of Mechanical Engineering at the Urmia University. His research interests include heat transfer and fluid mechanics.

Gholamreza Miri received his BSc and MSc degrees in Mechanical Engineering from Tabriz University in 1996 and 1998, respectively. His research interests include heat transfer and fluid mechanics.

Vahid Zare received his BSc, MSc, and PhD degrees in Mechanical Engineering from the Tabriz University in 2005, 2008, and 2013, respectively. He is currently an academic staff member at the Department of Mechanical Engineering at Urmia University of Technology. His research interests include exergy and fuel cells.